ChemComm

COMMUNICATION

View Article Online
View Journal | View Issue

Cite this: *Chem. Commun.*, 2014, **50**, 13698

Received 18th June 2014,
Accepted 15th September 2014

DOI: 10.1039/c4cc04615c

www.rsc.org/chemcomm

DNA-regulated silver nanoclusters for label-free ratiometric fluorescence detection of DNA†

Lin Liu, Qianhui Yang, Jianping Lei,* Nan Xu and Huangxian Ju

Two kinds of DNA-regulated Ag nanoclusters were one-pot synthesized on an oligonucleotide, and delicately utilized in the design of a label-free ratiometric fluorescence strategy for DNA detection with simplicity and high sensitivity.

Ratiometric fluorescence techniques have attracted much attention in the detection of complex samples through recording the ratio of fluorescence intensities at two different wavelengths.[1] Compared to steady-state fluorescence (FL), ratiometric fluorescence detection can minimize the environmental interfering factors, and thus more accurate and effective detection can be achieved.[2–6] There are two kinds of mechanisms generally utilized in ratiometric fluorescence detection. One is based on the emission change in response to the targets using organic dyes as fluorophores.[7–12] Typically, Lippard *et al.* have reported a red-emitting organic probe for turn-on and ratiometric fluorescence detection of Hg^{2+} in aqueous solution.[2] Kim *et al.* used a benzimidazole derivative as a ratiometric two-photon fluorescent probe to monitor acidic pH values by the change in emission color from blue to green.[9] The other mechanism is based on fluorescence resonance energy transfer (FRET) between the dye and nanomaterials.[13] By utilizing two kinds of fluorophores with energy donor–acceptor architectures larger pseudo-Stokes shifts can be achieved than by utilizing single fluorophores. For example, a specific ratiometric fluorescence technique was designed for detection of proteins through FRET between CdSe–ZnS core–shell quantum dots and a dye acceptor.[14] Although the above ratiometric fluorescence methods have achieved good performance for the detection of targets, the need for labeled fluorescent probes, poor anti-bleaching, or construction of donor–acceptor pairs have limited their applications in practice.

With the development of nanoscience and nanotechnology, fluorescence nanomaterials demonstrate some distinguished advantages in the design of ratiometric fluorescent probes. A binary heterogeneous nanocomplex of gold clusters and carbon dots was constructed for ratiometric detection of highly reactive oxygen species.[15] On the other hand, silver nanoclusters (Ag NCs) are promising options as fluorophores due to their regulative properties, especially for using DNA as a template. Since there is a high affinity between Ag^+ and a cytosine base (C base), Ag NCs could be generated directly from C-rich oligonucleotides by simple reduction of Ag^+, which allows the demission of labeling.[16] What is more, fluorescence properties of DNA-templated Ag NCs are largely sequence-,[17,18] and structure-dependent.[19–22] The formation of fluorescent Ag NCs in hybridized DNA duplex scaffolds can identify a typical single-nucleotide mutation.[23] Herein, using DNA as a template, two kinds of Ag NCs were one-pot synthesized on an oligonucleotide, and delicately utilized in the design of label-free ratiometric fluorescence strategy for DNA detection.

First, the sequence of probe 1 was delicately tailored to contain two regions (Scheme 1), which could simultaneously generate two kinds of silver nanoclusters (Ag NCs1 and Ag NCs2) with different fluorescence properties in the presence of $NaBH_4$. When target DNA was introduced, the red region of probe 1 could turn into a loop which enhanced the fluorescence intensity of Ag NCs1[23]

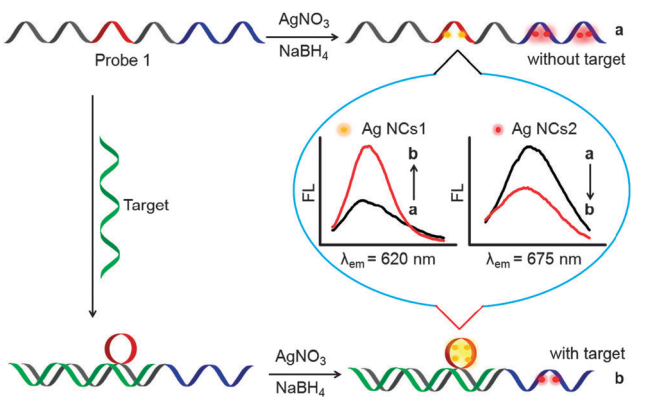

Scheme 1 Schematic illustration of a label-free ratiometric fluorescence strategy utilizing DNA-regulated Ag NCs for DNA detection.

State Key Laboratory of Analytical Chemistry for Life Science, School of Chemistry and Chemical Engineering, Nanjing University, Nanjing 210093, P. R. China. E-mail: jpl@nju.edu.cn; Fax: +86 25 83593593; Tel: +86 25 83593593

† Electronic supplementary information (ESI) available: Experimental details and additional figures. See DOI: 10.1039/c4cc04615c

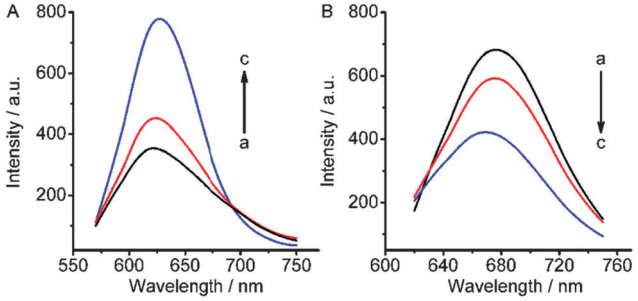

Fig. 1 Fluorescent spectra of (A) Ag NCs1 and (B) Ag NCs2 generated from 1 μM probe 1 (a), 1 μM probe 1 + 250 nM target DNA (b), and 1 μM probe 1 + 1 μM target DNA (c).

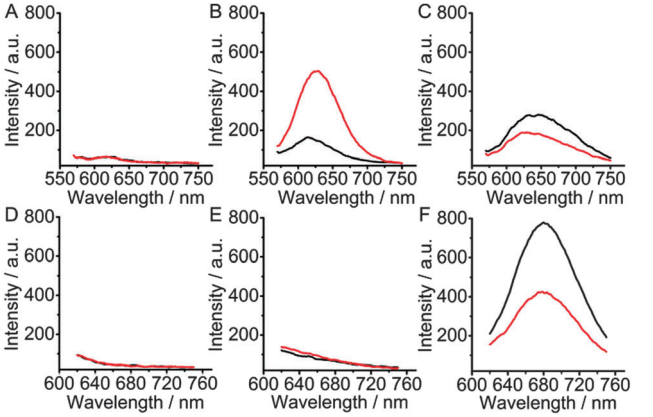

Fig. 2 Fluorescence spectra of (A–C) Ag NCs1 and (D–F) Ag NCs2 generated by utilizing 1 μM probe X (A and D), probe R (B and E) and probe B (C and F) with (red line) and without (black line) 1 μM target DNA.

while the fluorescence intensity of Ag NCs2 originating from the blue region decreased. The ratios of two fluorescence intensities at different emission wavelengths could be used to quantify the concentration of target DNA in a sensitive way.

The feasibility of the proposed method was identified by the spectral change in response to targets. Probe 1 (1 μM) alone demonstrated two emission peaks at 620 nm and 675 nm with excitation wavelengths of 550 nm and 600 nm for Ag NCs1 and Ag NCs2, respectively (Fig. S1, ESI†). With the increasing of target DNA concentrations, the fluorescence intensity of Ag NCs1 (F_{620}) was greatly enhanced (Fig. 1A, curves b and c) while the fluorescence intensity of Ag NCs2 (F_{675}) was obviously reduced (Fig. 1B, curves b and c). The opposite change in fluorescence intensities led to the large ratios of F_{620}/F_{675} for ratiometric fluorescence detection of target DNA with convenience and sensitivity.

To identify the functions of the sequences in red and blue regions, three kinds of probes were designed for generation of the fluorescent Ag NCs (Table 1). First, for probe X, which was just a complementary oligonucleotide of target DNA, no fluorescence emissions were observed in the presence/absence of target DNA (Fig. 2A and D). This result suggested that the sequence of probe X could not template the generation of fluorescent Ag NCs even in the presence of abundant C bases. Second, probe R containing the red part more than probe X, could only generate Ag NCs1 alone as predicted (Fig. 2B and E, black). Adding target DNA to probe R caused a dramatic increase in the fluorescence intensity of Ag NCs1 (Fig. 2B, red), because the red part turned into a loop to enhance fluorescence emission.[23] As for the probe (probe B) containing the blue part more than probe X, strong fluorescence emission of Ag NCs2 was observed along with weak fluorescence emission of Ag NCs1 (Fig. 2C and F, black). However, after hybridizing with the target, the fluorescence intensities of both Ag NCs1 and Ag NCs2 reduced obviously due to the formation of the duplex, which was consistent with the previous report.[24] Therefore, it could be inferred that the conformation of red and blue regions regulated the generation of Ag NCs, providing a possibility in the design of a label-free ratiometric fluorescence method for detection of DNA.

To analyze the internal relationship between the sequence of the loop and Ag NCs1, the probes with different loop sequences were studied (Table S1, ESI†). Probe RA, which was designed by deleting base A from the loop of probe R, could not generate any fluorescent Ag NCs in the presence/absence of target DNA (Fig. S2, black, ESI†), showing that base A in the loop was important for the generation of the fluorescent Ag NCs. Subsequently, by replacing base A with G, T and C bases, probe RG, probe RT and probe RC were designed, respectively. Probes RG and RT could not lead to fluorescence intensity obviously different from probe RA (Fig. S2, green and blue, ESI†) while probe RC generated strong fluorescence emission of Ag NCs1 (Fig. S2, red, ESI†). However, for probe RC, introduction of the target could not lead to an obvious fluorescence enhancement. Therefore, the A base in the loop was no substitute in the design of the probe for ratiometric fluorescence detection.

In order to obtain good performance, the concentration of probe 1, vibrating time of $NaBH_4$ and pH during synthesis of Ag NCs were optimized. As shown in Fig. S3A (ESI†), the fluorescence intensity increased linearly along with the concentrations of probe 1. Considering the accuracy and economy of detection,

Table 1 Oligonucleotides employed in this work

Oligonucleotides	Oligonucleotides sequence (5′–3′)
Probe 1	TATTAACTTTACTCCCTTACCCTTCCTCCCCGCTGATTTTCCCCTTTT
Target	TCAGCGGGGAGGAAGGGAGTAAAGTTAATA
Probe B	TATTAACTTTACTCCCTTCCTCCCCGCTGATTTTCCCCTTTT
Probe R	TATTAACTTTACTCCCTTACCCTTCCTCCCCGCTGA
Probe X	TATTAACTTTACTCCCTTCCTCCCCGCTGA

The red and blue parts of probes represent the loop and 3′-end sequences for generating two different kinds of Ag NCs, respectively.

1 μM was chosen as the optimal concentration of probe 1 in the detection procedure. The vibrating time of $NaBH_4$ was also optimized in the range of 3 to 30 min. Obviously, the vibrating time of 15 min resulted in a large difference of fluorescence ratios for two Ag NCs (Fig. S3B, ESI†). pH during synthesis of Ag NCs was an important factor to affect the fluorescence intensity of DNA-regulated Ag NCs. The fluorescence ratio of Ag NCs1 increased with an increase of pH from 6.5 to 8.0, while the fluorescence ratio of Ag NCs2 decreased with an increase of pH up to 7.5 (Fig. S3C, ESI†). Therefore, 20 mM Tris-HCl buffer of pH 7.5 was used throughout the following experiments.

The synthesized Ag NCs were characterized by transmission electron microscopy. The size of Ag NCs1 generated from probe B is slightly smaller than that generated from probe R (~2 nm) with homogeneous distribution (Fig. S4B and C, ESI†). In addition, the higher density Ag NCs originating from probe 1 were observed (Fig. S4A, ESI†). These results identified the formation of two different Ag NCs on the DNA template.

Under the optimized conditions, target DNA of different concentrations from 0 to 1000 nM was detected. The ratio of fluorescence intensities was proportional to the target concentration ranging from 10 to 1000 nM (Fig. 3). The linear regression equation was $I = 0.515 + 0.00134 \times c$ ($R^2 = 0.991$), where I is the ratio of fluorescence intensities of Ag NCs1 and Ag NCs2, and c is the concentration of target DNA. The limit of detection at 3σ calculated in the absence of the target was estimated to be 7.3 nM, which was lower than those calculated by steady-state fluorescence DNA sensing strategies using DNA-templated Ag NCs[25,26] or ratiometric fluorescence methods.[7]

The specificity of this ratiometric fluorescence strategy combining Ag NCs was demonstrated to be acceptable for discriminating the three-base mismatched DNA from the complementary target (Fig. S5, ESI†). Also, the positions of the mismatched bases could be figured out by comparing the changes in fluorescence intensities of Ag NCs1 and Ag NCs2. When the mismatched bases were near the loop (Table S1, R-tm target, ESI†), which might influence the formation of the loop, the enhancement of fluorescence intensity of Ag NCs1 caused by the R-tm target was only as much as 25% of the same concentration complementary target. Meanwhile, the R-tm target had no effect on the formation of Ag NCs2. Similarly, when the mismatched bases were near the blue region (Table S1, B-tm target, ESI†), the decrease of fluorescence intensity of Ag NCs2 was as much as 60% of the same concentration complementary target, and the enhancement of fluorescence intensity of Ag NCs1 was the same as that observed with the complementary target. The ratiometric strategy can enlarge the difference between mismatch DNA and target DNA. Thus the dual fluorescence change provides a reliable method for discriminating the mismatched DNA in DNA detection.

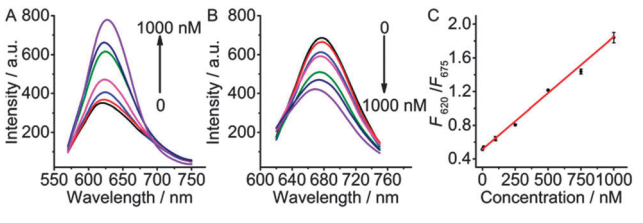

Fig. 3 Fluorescence spectra of (A) Ag NCs1 and (B) Ag NCs2 using 1 μM probe 1 as a template at 0, 10, 100, 250, 500, 750, and 1000 nM target concentrations. (C) The calibration curve of fluorescence intensity ratio of F_{620} to F_{675} *vs.* target DNA concentration.

To test the validity of the proposed assay in clinical samples, recovery testing was carried out by spiking the target DNA solution into human serum. At a concentration of 500 nM, the recovery was 92.0 ± 2.9% (n = 3), indicating that the proposed ratiometric strategy for DNA detection could be used in real sample analysis.

In this work we developed a label-free ratiometric fluorescence strategy based on DNA-regulated Ag nanoclusters for sensitive detection of DNA. By regulating the conformation of the probe, two kinds of Ag NCs were successfully one-pot prepared with different fluorescence properties. Upon introducing target DNA, the red region turned into a loop so that the fluorescence intensity of Ag NCs1 was enhanced. Meanwhile, fluorescence intensity of Ag NCs2 decreased due to the formation of a duplex. The opposite change led to the large ratios of two fluorescence intensities from Ag NCs, and thus was used to sensitively quantify target DNA in a ratiometric way. Interestingly, the mismatched bases could be effectively positioned by comparing the fluorescence changes in Ag NCs1 and Ag NCs2. In addition, the different sequence of the loop resulted in a different fluorescence response to the targets, and thus this phenomenon shows potential for distinguishing single nucleotide polymorphism. The nanomaterial-based ratiometric fluorescence method can overcome the disadvantages of the organic fluorescent probe, and expand the application of fluorescence detection in bioimaging and bioanalysis.

This research was financially supported by the National Basic Research Program of China (2010CB732400) and the National Natural Science Foundation of China (21375060, 21135002, and 21121091).

Notes and references

1 (*a*) J. L. Fan, M. M. Hu, P. Zhan and X. J. Peng, *Chem. Soc. Rev.*, 2013, **42**, 29–43; (*b*) K. M. Wang, X. X. He, X. H. Yang and H. Shi, *Acc. Chem. Res.*, 2013, **46**, 1367–1376; (*c*) K. Kikuchi, *Chem. Soc. Rev.*, 2010, **39**, 2048–2053; (*d*) C. J. Chang, J. Jaworski, E. M. Nolan, M. Sheng and S. J. Lippard, *Proc. Natl. Acad. Sci. U. S. A.*, 2004, **101**, 1129–1134; (*e*) G. Q. Zhang, G. M. Palmer, M. W. Dewhirst and C. L. Fraser, *Nat. Mater.*, 2009, **8**, 747–751.
2 E. M. Nolan and S. J. Lippard, *J. Am. Chem. Soc.*, 2007, **129**, 5910–5918.
3 X. F. Hou, Q. X. Yu, F. Zeng, C. M. Yu and S. Z. Wu, *Chem. Commun.*, 2014, **50**, 3417–3420.
4 C. M. Yu, X. Z. Li, F. Zeng, F. Y. Zheng and S. Z. Wu, *Chem. Commun.*, 2013, **49**, 403–405.
5 C. Q. Ding, A. W. Zhu and Y. Tian, *Acc. Chem. Res.*, 2013, **47**, 20–30.
6 A. W. Zhu, Q. Qu, X. L. Shao, B. Kong and Y. Tian, *Angew. Chem., Int. Ed.*, 2012, **124**, 7297–7301.
7 L. M. Huang and S. W. Tam-Chang, *Chem. Commun.*, 2011, **47**, 2291–2293.
8 T. Yoshihara, Y. Yamaguchi, M. Hosaka, T. Takeuchi and S. Tobita, *Angew. Chem., Int. Ed.*, 2012, **51**, 4148–4151.
9 H. J. Kim, C. H. Heo and H. M. Kim, *J. Am. Chem. Soc.*, 2013, **135**, 17969–17977.
10 E. G. Matveeva, Z. Gryczynski, D. R. Stewart and I. Gryczynski, *J. Lumin.*, 2009, **129**, 1281–1285.

11 J. Ueberfeld and D. R. Walt, *Anal. Chem.*, 2004, **76**, 947–952.
12 P. J. Santangelo, B. Nix, A. Tsourkas and G. Bao, *Nucleic Acids Res.*, 2004, **32**, e57.
13 (*a*) X. J. Liu, N. Zhang, T. Bing and D. H. Shangguan, *Anal. Chem.*, 2014, **86**, 2289–2296; (*b*) C. M. Tyrakowski and P. T. Snee, *Anal. Chem.*, 2014, **86**, 2380–2386; (*c*) J. F. Han, C. Zhang, F. Liu, B. H. Liu, M. Y. Han, W. S. Zou, L. Yang and Z. P. Zhang, *Analyst*, 2014, **139**, 3032–3038; (*d*) Y. Zhou, W. B. Pei, C. Y. Wang, J. X. Zhu, J. S. Wu, Q. Y. Yan, L. Huang, W. Huang, C. Yao, J. S. C. Loo and Q. C. Zhang, *Small*, 2014, **10**, 3560–3567.
14 H. Y. Zhang, G. Q. Feng, Y. Guo and D. J. Zhou, *Nanoscale*, 2013, **5**, 10307–10315.
15 E. G. Ju, Z. Liu, Y. D. Du, Y. Tao, J. S. Ren and X. G. Qu, *ACS Nano*, 2014, **8**, 6014–6023.
16 J. T. Petty, J. Zheng, N. V. Hud and R. M. Dickson, *J. Am. Chem. Soc.*, 2004, **126**, 5207–5212.
17 B. Sengupta, C. M. Ritchie, J. G. Buckman, K. R. Johnsen, P. M. Goodwin and J. T. Petty, *J. Phys. Chem. C*, 2008, **112**, 18776–18782.
18 J. Sharma, R. C. Rocha, M. L. Phipps, H. Yeh, K. A. Balatsky, D. M. Vu, A. P. Shreve, J. H. Werner and J. S. Martinez, *Nanoscale*, 2012, **4**, 4107–4110.
19 Z. X. Zhou, Y. Q. Liu and S. J. Dong, *Chem. Commun.*, 2013, **49**, 3107–3109.
20 L. Y. Feng, Z. Z. Huang, J. S. Ren and X. G. Qu, *Nucleic Acids Res.*, 2012, **40**, e122.
21 B. Sengupta, K. Springer, J. G. Buckman, S. P. Story, O. H. Abe, Z. W. Hasan, Z. D. Prudowsky, S. E. Rudisill, N. N. Degtyareva and J. T. Petty, *J. Phys. Chem. C*, 2009, **113**, 19518–19524.
22 T. Li, L. B. Zhang, J. Ai, S. J. Dong and E. K. Wang, *ACS Nano*, 2011, **5**, 6334–6338.
23 W. W. Guo, J. P. Yuan, Q. Z. Dong and E. K. Wang, *J. Am. Chem. Soc.*, 2010, **132**, 932–934.
24 (*a*) S. W. Yang and T. Vosch, *Anal. Chem.*, 2011, **83**, 6935–6939; (*b*) P. Shah, P. W. Thulstrup, S. K. Cho, Y. J. Bhang, J. C. Ahn, S. W. Choi, M. J. Bjerrum and S. W. Yang, *Analyst*, 2014, **139**, 2158–2166; (*c*) P. Shah, A. Rørvig-Lund, S. B. Chaabane, P. W. Thulstrup, H. G. Kjaergaard, E. Fron, J. Hofkens, S. W. Yang and T. Vosch, *ACS Nano*, 2012, **6**, 8803–8814.
25 L. B. Zhang, J. B. Zhu, Z. X. Zhou, S. J. Guo, J. Li, S. J. Dong and E. K. Wang, *Chem. Sci.*, 2013, **4**, 4004–4010.
26 G. Y. Lan, W. Y. Chen and H. T. Chang, *Biosens. Bioelectron.*, 2011, **26**, 2431–2435.